Shilin Chen
Michel Géradin
Aerospace Laboratory (LTAS)
University of Liège
21 Rue E. Solvay
4000 Liège, Belgium

Exact and Direct Modeling Technique for Rotor-Bearing Systems with Arbitrary Selected Degrees-of-Freedom

An exact and direct modeling technique is proposed for modeling of rotor-bearing systems with arbitrary selected degrees-of-freedom. This technique is based on the combination of the transfer and dynamic stiffness matrices. The technique differs from the usual combination methods in that the global dynamic stiffness matrix for the system or the subsystem is obtained directly by rearranging the corresponding global transfer matrix. Therefore, the dimension of the global dynamic stiffness matrix is independent of the number of the elements or the substructures. In order to show the simplicity and efficiency of the method, two numerical examples are given.

INTRODUCTION

The subject of rotor-bearing dynamics has received considerable attention over the last few decades. The reason for this interest in rotor-bearing dynamics is almost certainly the demand placed on manufacturers to continuously improve both the power rating and the reliability of rotating machinery (Goodwin, 1992). For dynamic analysis, modeling of the rotor-bearing systems is the first step. Various methods for modeling rotor-bearing systems have been developed and widely used during the past few decades. Among these techniques, the transfer matrix method (TMM) and the finite element method (FEM) may be most commonly used for multi-degree-of-freedom (MDOF) rotor-bearing systems.

The outstanding advantage of the TMM is that it requires calculations using matrices of fixed size, irrespective of the number of DOF in the problem. This means that the computational complexity is low even when dealing with systems with hundreds of DOF. However, only the natural frequencies, mode shapes, and harmonic response are available so far by this method. The other important modal parameters such as modal mass, modal stiffness, and transfer function of the system cannot be obtained. Furthermore, the stiffness and mass matrices that are important for modeling the systems are not available when the TMM is used.

At the current state of rotor dynamic technology, the FEM has proved to be powerful and versatile. It is also the only validated tool available at the present time for nonlinear systems and for transient dynamic analysis. However, in this method, the number of DOF is very high for large rotor-bearing systems. Many unwanted DOF such as rotational and internal DOF are used in the model. This makes it difficult for the FEM model to compare with the experimental model due to the large difference in the numbers of coordinates used in both models. If such com-

Received February 10, 1994; Accepted April 22, 1994.
Shock and Vibration, Vol. 1, No. 6, pp. 497–506 (1994)

CCC 1070-9622/94/060497-10

parison is necessary, the FEM model has to be reduced, which may be uneconomical in some cases.

Another alternative is the dynamic stiffness matrix method (DSM). It may be considered as an improved FEM. Being different from the FEM, the DSM uses the analytical solutions of the governing equations as shape functions. Therefore, the obtained DSM is exact in the sense of the exact governing equation. These matrices are in general parametric in terms of the vibration frequency and the load factor.

One of the most important advantages of the DSM is that the DOF needed to model a structure is significantly reduced compare to the FEM. This is due to the fact that a uniform shaft, for example, can be taken as long as needed in the DSM. There is a significant number of references describing the method. Fergusson and Pilkey (1991a,b, 1993a,b) have reviewed the relevant literature up to 1992. Most of the literature up to the end of 1992 may be found in their reviews.

However, there are some drawbacks associated with the DSM. First, the number of DOF is still high for large structures. Similarly to the FEM, many unwanted DOF such as rotational degrees remain in the model. Second, the calculation of modal parameters requires the solution of a highly nonlinear (trascendental) eigenproblem:

$$[D(\omega)]X = 0.$$

To this purpose, some special algorithms should be used, for example, the algorithms described by Williams and Wittrick (1970), Wittrick and Williams (1971), and Richards and Leung (1977). The former algorithm requires calculation of natural frequencies for each individual beam element with its end fixed. This increases the computational time significantly.

In order to minimize the dynamic DOF without any loss of accuracy, a combination method was introduced by Dokainish (1972) for plate vibration problems in which the element transfer matrix was obtained directly from the element stiffness and mass matrices. In recent years, this combination method has been improved by other researchers (Chiatti and Sestieri, 1979; Ohga et al., 1983; Degen et al., 1985) for different applications. In this method, the eigenfrequencies and mode shapes are calculated from the global transfer matrix. Therefore, it may be considered as an improved transfer matrix method with application to plates. However, for rotor-bearing systems it seems to be unnecessary to obtain the element transfer matrix from the element stiffness and mass matrices because the element transfer matrix may be derived directly from the governing equations in an exact manner (Lund and Orcutt, 1967; Lee et al., 1991).

For rotor-bearing systems, the idea of combining the TMM and FEM to reduce the DOF was first proposed by Dimarogonas (1975). A static deflection function between nodes were used in his article. This idea was used for stability analysis of a rotating shaft.

In this article an exact and direct modelling technique for rotor-bearing systems based on the combination of transfer and dynamic stiffness matrices is presented. In this technique, the entire structure is first divided into several substructures based on the required master DOF. Each substructure may consist of a large number of basic elements. The DOF for a substructure may be partitioned into two sets. One set is the internal DOF, and the other set is the boundary DOF. The transfer matrix of each substructure relates only the boundary DOF. The dynamic stiffness matrix of the substructure is obtained by rearranging the corresponding transfer matrix. In this way, the internal DOF are not used in the model. In other words, a substructure is reduced exactly to an equivalent element whose nodal coordinates are the boundary coordinates of the substructure. The boundary coordinates dynamic stiffness matrices of substructures become the basic matrices for assembling the global dynamic stiffness matrix for the original structure. The order of the system eigenvalue equation is equal to the number of physical boundary coordinates between substructures and is frequency dependent. Because the dynamic stiffness matrices of the basic elements such as shaft, lumped mass, and stiffness elements are exact, the number of modes predicted by the model is not limited by the number of master DOF used in the model.

The consistent equations of motion of a rotating Timoshenko shaft subject to axial force derived recently by Choi et al. (1992) are used as the governing equations. In the equations, the effects of rotary inertia, gyroscopic, and transverse shear are taken into account. An exact transfer matrix for the shaft is derived directly from the governing equations following the procedure proposed by Lee et al. (1991). The rotor-bearing system is then reduced to a low dimension model with arbitrary selected DOF. All modal parameters of the rotor-bearing systems such as eigenfrequencies, mode shapes, modal masses, modal stiffness, and frequency response functions can be obtained from the established model. Two numerical examples are given to show the simplicity and high accuracy of the method. As a by-product, the exact dynamic stiffness matrix for a rotating shaft subject to axial force can be obtained by rearranging the corresponding exact transfer matrix using the technique described here.

DERIVATION OF EXACT TRANSFER MATRIX FOR A SHAFT

Governing Equations

Let us first examine a uniform shaft subject to constant compression axial load as shown in Fig. 1. For such a shaft, the consistent equations of motion have been derived recently using the finite strain beam theory (Choi et al., 1992). In the XZ plane:

$$\begin{aligned}\frac{\partial^4 X}{\partial Z^4} - \left(\frac{\rho}{KG} + \frac{\rho}{E}\right)\frac{\partial^4 X}{\partial Z^2 \partial t^2} + \frac{\rho^2}{KEG}\frac{\partial^4 X}{\partial t^4} + \frac{\rho A}{EI}\frac{\partial^2 X}{\partial t^2} - \frac{2\rho\omega}{E}\left(\frac{\partial^3 Y}{\partial Z^2 \partial t} - \frac{\rho}{KG}\frac{\partial^3 Y}{\partial t^3}\right) \\ + \frac{P}{EI}\left(1 + \frac{P}{KAG}\right)\frac{\partial^2 X}{\partial Z^2} + \frac{\rho P}{EIKG}\frac{\partial^2 X}{\partial t^2} - \frac{P^2}{E^2 AI}\frac{\partial^2 X}{\partial Z^2} + \left(-\frac{2P}{EA} - \frac{P^2}{EAKAG} + \frac{P^2}{(EA)^2}\right)\frac{\rho A}{EI}\frac{\partial^2 X}{\partial t^2} = 0.\end{aligned} \tag{1a}$$

In the YZ plane:

$$\begin{aligned}\frac{\partial^4 Y}{\partial Z^4} - \left(\frac{\rho}{KG} + \frac{\rho}{E}\right)\frac{\partial^4 Y}{\partial Z^2 \partial t^2} + \frac{\rho^2}{KEG}\frac{\partial^4 Y}{\partial t^4} + \frac{\partial A}{EI}\frac{\partial^2 Y}{\partial t^2} + \frac{2\rho\omega}{E}\left(\frac{\partial^3 X}{\partial Z^2 \partial t} - \frac{\rho}{KG}\frac{\partial^3 X}{\partial t^3}\right) \\ + \frac{P}{EI}\left(1 + \frac{P}{KAG}\right)\frac{\partial^2 Y}{\partial Z^2} + \frac{\rho P}{EIKG}\frac{\partial^2 Y}{\partial t^2} - \frac{P^2}{E^2 AI}\frac{\partial^2 Y}{\partial Z^2} + \left(-\frac{2P}{EA} - \frac{P^2}{EAKAG} + \frac{P^2}{(EA)^2}\right)\frac{\rho A}{EI}\frac{\partial^2 Y}{\partial t^2} = 0\end{aligned} \tag{1b}$$

with the following quantities: E is the Young's modulus, G the shear modulus, K the shear factor, ρ the mass density, A the cross section area, and P the axial compression load. It is noted that not only the gyroscopic moments but also the axial load terms are consistently captured in the above equations.

Transfer Matrix for a Shaft

The steady-state solutions of Eq. (1) may be represented in the form

$$\begin{aligned} X(Z, t) &= X_s(Z)\sin \Omega t \\ Y(Z, t) &= Y_c(Z)\cos \Omega t \end{aligned} \tag{2}$$

where Ω is the whirling angular frequency.

Substituting Eqs. (2) into (1) would result in two homogeneous equations as follows. In the XZ plane

$$\begin{aligned}\frac{d^4 X_s}{dZ^4} + \left(\frac{\rho\Omega^2}{E} + \frac{\rho\Omega^2}{KG}\right)\frac{d^2 X_s}{dZ^2} + \left(\frac{\rho^2\Omega^4}{KGE} - \frac{\rho A\Omega^2}{EI}\right)X_s + \frac{2\rho\omega\Omega}{E}\frac{d^2 Y_c}{dZ^2} + \frac{2\rho^2\omega\Omega^3}{KGE}Y_c \\ + \frac{P}{EI}\left(1 + \frac{P}{KAG}\right)\frac{d^2 X_s}{dZ^2} - \frac{\rho P\Omega^2}{EIKG}X_s - \frac{P^2}{E^2 AI}\frac{d^2 X_s}{dZ^2} - \frac{\rho A\Omega^2}{EI}\left(-\frac{2P}{EA} - \frac{P^2}{EAKAG} + \frac{P^2}{(EA)^2}\right)X_s = 0.\end{aligned} \tag{3a}$$

In the YZ plane

$$\begin{aligned}\frac{d^4 Y_c}{dZ^4} + \left(\frac{\rho\Omega^2}{E} + \frac{\rho\Omega^2}{KG}\right)\frac{d^2 Y_c}{dZ^2} + \left(\frac{\rho^2\Omega^4}{KGE} - \frac{\rho A\Omega^2}{EI}\right)Y_c + \frac{2\rho\omega\Omega}{E}\frac{d^2 X_s}{dZ^2} + \frac{2\rho^2\omega\Omega^3}{KGE}X_s \\ + \frac{P}{EI}\left(1 + \frac{P}{KAG}\right)\frac{d^2 Y_c}{dZ^2} - \frac{\rho P\Omega^2}{EIKG}Y_c + \frac{P^2}{E^2 AI}\frac{d^2 Y_c}{dZ^2} - \frac{\rho A\Omega^2}{EI}\left(-\frac{2P}{EA} - \frac{P^2}{EAKAG} + \frac{P^2}{(EA)^2}\right)Y_c = 0.\end{aligned} \tag{3b}$$

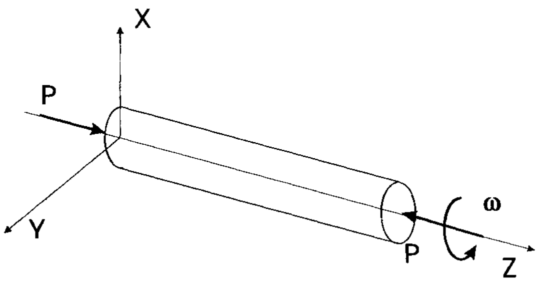

FIGURE 1 Rotating Timoshenko shaft subject to axial load.

The solutions of Eqs. (3) take the form

$$X_s = U_s e^{\lambda Z}$$
$$Y_c = V_c e^{\lambda Z} \tag{4}$$

where U_s, V_c are arbitrary real constants and λ are the roots of the determinant equation

$$\begin{vmatrix} \lambda^4 + f\lambda^2 + g & h\lambda^2 + k \\ h\lambda^2 + k & \lambda^4 + f\lambda^2 + g \end{vmatrix} = 0 \tag{5}$$

with

$$f = \frac{\rho\Omega^2}{E} + \frac{\rho\Omega^2}{KG} + \frac{P}{EI} + \frac{P^2}{KAGEI} - \frac{P^2}{E^2AI}$$

$$g = \frac{\rho^2\Omega^4}{KGE} - \frac{\rho A\Omega^2}{EI} - \frac{\rho P\Omega^2}{EIKG} + \frac{\rho A}{EI}\frac{2P\Omega^2}{EA} + \frac{\rho P^2\Omega^2}{E^2IAKG} - \frac{P^2\rho\Omega^2}{E^3AI}$$

$$h = \frac{2\rho\omega\Omega}{E}, \quad k = \frac{2\rho^2\omega\Omega^3}{KGE}.$$

Equation (5) is equivalent to the following equations:

$$\lambda^4 - b_1\lambda^2 + c_1 = 0 \tag{5a}$$

$$\lambda^4 - b_2\lambda^2 + c_2 = 0 \tag{5b}$$

where $b_1 = h - f$, $c_1 = g - k$, $b_2 = -(f + h)$, $c_2 = g + k$.

Let us consider first Eq. (5a). The following two cases are considered.

Case 1. $\sqrt{b_1^2 - 4c_1} > b_1$. This is true for $c_1 < 0$. Physically, this case would correspond to lower frequency vibrations. A numerical test has shown that this is the case for most rotor-bearing systems. The solutions for λ are given by:

$$\lambda = \pm i\lambda_1, \pm\lambda_2$$

in which

$$\lambda_1 = \sqrt{\frac{-b_1 + \sqrt{b_1^2 - 4c_1}}{2}}$$

$$\lambda_2 = \sqrt{\frac{b_1 - \sqrt{b_1^2 - 4c_1}}{2}}$$

Case 2. $\sqrt{b_1^2 - 4c_1} < b_1$. This is true for $b_1 > 0$, and $c_1 > 0$. Physically, this case would correspond to higher frequency vibrations. The solutions of Eq. (5b) in this case are given by:

$$\lambda = \pm\lambda_1, \pm\lambda_2$$

in which

$$\lambda_1 = i\lambda_2 = \sqrt{\frac{b_1 - \sqrt{b_1^2 - 4c_1}}{2}}.$$

The numerical test has shown that this case may happen only at very high frequency. This is not the case for most industrial rotors.

Combining the above two cases, the roots of the characteristic function of Eq. (5) may take the form:

$$\lambda = \pm\lambda_a, \pm i\lambda_b, \pm\lambda_c, \pm i\lambda_d$$

for a constant value of ω (see also Lee et al., 1991; Zu and Han, 1992).

In the same way as the displacements, the slopes, moments, and shear forces may be defined as follows:

$$\begin{aligned} \alpha(Z, t) &= \alpha_s(Z)\sin\Omega t \\ \beta(Z, t) &= \beta_c(Z)\cos\Omega t \\ M_x(Z, t) &= M_{xs}(Z)\sin\Omega t \\ M_y(Z, t) &= M_{yc}(Z)\cos\Omega t \\ Q_x(Z, t) &= Q_{xs}(Z)\sin\Omega t \\ Q_y(Z, t) &= Q_{yc}(Z)\cos\Omega t. \end{aligned} \tag{6}$$

The state vector is defined as follows:

$$S = [X_s, Y_c, \alpha_s, \beta_c, M_{xs}, M_{yc}, Q_{xs}, Q_{yc}]^t.$$

The state vector on the right-hand side of the shaft is related to the state vector on the left-hand side by the following matrix equation:

$$S_i = [T]S_{i-1} \tag{7}$$

where $[T]$ is the transfer matrix of a shaft element with dimension 8×8 and

$$[T] = [A]^{-1}[N][A]. \tag{8}$$

The matrices [A] and [N] are given in the Appendix.

GLOBAL FREQUENCY-DEPENDENT MATRICES

Substructure Transfer Matrix

A typical substructure is shown in Fig. 2 that consists of N_k elastic supports, N_m lumped masses, N_d rigid disks, and N_b beam elements.

The global transfer matrix for the substructure is:

$$[T] = [T_N][T_{N-1}] \cdot \cdot \cdot [T_2][T_1] \tag{9}$$

where N is the total number of elements and $N = N_b + N_k + N_m + N_d$. It should be noted that although the shaft element length may be taken as long as possible in the case of uniform cross section because of the use of the exact transfer matrix, the total number of elements of a substructure or the entire structure may still be large for very long rotor systems. In this case, numerical instability due to matrix multiplication may occur. This difficulty may be overcome by using symbolic computation, for example the Maple software. On the other hand, if N is very large, a lot of matrix multiplication is needed. To speed up the calculation, parallel algorithms may be used.

Substructure Dynamic Stiffness Matrix

The global transfer matrix $[T]$ of a substructure relates the forces and displacements at both ends of the substructure in the following way:

$$\begin{pmatrix} X_r \\ -F_r \end{pmatrix} = \begin{pmatrix} T_{11} & T_{12} \\ T_{21} & T_{22} \end{pmatrix} \begin{pmatrix} X_l \\ F_l \end{pmatrix} \tag{10}$$

where F_l and X_l are the force and displacement vectors at the left end of the substructure, F_r and X_r are the same quantities at the right end. Equation (10) may be rewritten in the dynamic stiffness matrix form:

$$\begin{pmatrix} F_l \\ F_r \end{pmatrix} = \begin{pmatrix} D_{11} & D_{12} \\ D_{21} & D_{22} \end{pmatrix} \begin{pmatrix} X_l \\ X_r \end{pmatrix} \tag{11}$$

with

$$D_{11} = -T_{12}^{-1}T_{11}$$
$$D_{12} = T_{12}^{-1}$$
$$D_{21} = -T_{21} + T_{22}T_{12}^{-1}T_{11}$$
$$D_{22} = -T_{22}T_{12}^{-1}$$

where $[D]$ is the global dynamic stiffness matrix of the substructure whose elements are frequency dependent. Note that the global dynamic stiffness matrix of the substructure has the same dimension as the element transfer matrix.

Equation (11) tells us that the substructure shown in Fig. 2 is reduced to an equivalent element whose nodal coordinates are the boundary coordinates of the substructure. The internal coordinates of the substructure are not used in Eq. (11).

Global Dynamic Stiffness Matrix

The global dynamic stiffness matrix for the entire structure can be assembled using the above dynamic stiffness matrices of all substructures. Af-

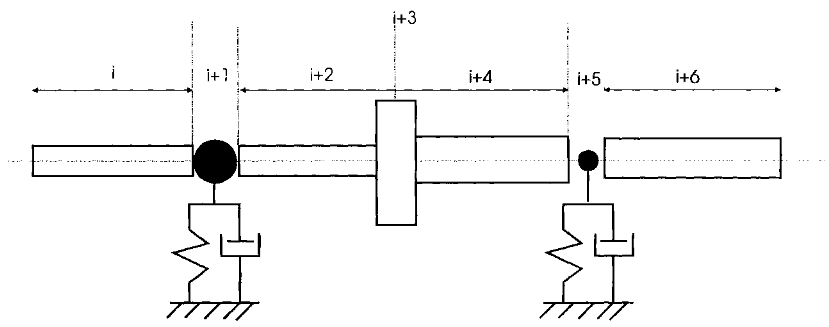

FIGURE 2 A substructure.

ter introducing the boundary conditions at both ends, the dimension of the global stiffness matrix can further be decreased. The restrained global dynamic stiffness matrix is denoted by $[D_g]$. The unwanted DOF such as rotational DOF can be removed in an exact manner as shown in the following numerical examples.

It is of interest to note that the global dynamic stiffness matrix obtained in this way is very low in dimension. It uses only the boundary coordinates of the substructures as the DOF. The internal DOF are not contained in the model. It should be pointed out that if the selected DOF happen to be the boundary coordinates of the entire structure, then only one substructure is needed and all the internal DOF are not contained in the model.

Global Frequency-Dependent Matrices

The global frequency-dependent matrices, that is, mass matrix, $[M]$, gyroscopic matrix $[G]$, and stiffness matrix, $[K]$, may be obtained from the global dynamic stiffness matrix $[D_g]$ (Richards and Leung, 1977; Yang and Pilkey, 1992; Leung and Fergusson, 1993):

$$[M_g(\omega, \Omega)] = -\frac{d[D_g(\omega, \Omega)]}{d(\Omega^2)} \tag{12a}$$

$$[G_g(\omega, \Omega)] = -\frac{d[D_g(\omega, \Omega)]}{d(\Omega)} \tag{12b}$$

$$[K_g(\omega, \Omega)] = \Omega^2[M_g(\omega, \Omega)] + i\Omega[G_g(\omega, \Omega)] + [D_g(\omega, \Omega)]. \tag{12c}$$

Modal Parameter Evaluation

Once the global dynamic stiffness matrix $[D_g]$ of the system is obtained, the natural frequencies are those values of Ω (for a given rotation speed ω) for which

$$[D_g(\omega, \Omega)]X = 0. \tag{13}$$

There are many ways to solve this nonlinear eigenvalue problem. Because $[D_g]$ is a very low dimension matrix, Eq. (13) can be solved by a straightforward procedure of calculating $\det[D_g(\omega, \Omega)]$ at many closely spaced Ω values within the frequency band of interest, taking the two values that bracket each sign change, and then iteratively calculating each 0 crossing ω_n value between the bracketed values.

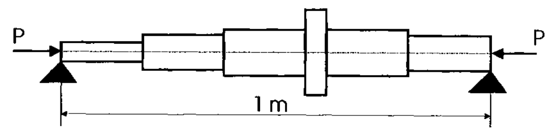

FIGURE 3(a) Simply supported rotor with a disk.

The modal mass for mode n may be obtained by (Richards and Leung, 1977):

$$M_s^n = X_n^T[M(\Omega_n)]X_n. \tag{14}$$

The response to harmonic excitation at any frequency Ω can be easily obtained in this stage. In fact, $[D_g(\Omega)]^{-1}$ is the exact frequency response function (FRF) matrix for the given DOF.

NUMERICAL EXAMPLES

Example 1: Simply Supported Rotor with Disk

The simply supported rotor with a disk subject to axial force shown in Fig. 3(a) is studied as the first example. The geometric parameters of the system are also given in the figure. The material of the rotor is steel with Poisson's ratio $\mu = 0.3$, Young's modulus $E = 2.1 \times 10^1$ 1 N/m and mass density $\rho = 7800$ kg/m^3. The purpose is to model this rotor to 2DOF with the translational displacements X_2 and Y_2 at the disk as the generalized coordinates.

The six basic elements (five shaft elements and one disk element) may be represented by two substructures as shown in Fig. 3(b). The transfer matrices $[T_1]$, $[T_2]$ for each substructure are easily obtained. Their corresponding dynamic stiffness matrices $[D_1]$, $[D_2]$ are obtained by rearranging the matrices $[T_1]$, $[T_2]$ according to Eq. (11).

The global dynamic stiffness matrix $[D]$ for the entire rotor system may be obtained by applying the standard assembly procedure of the finite element method. It is noted that the obtained unre-

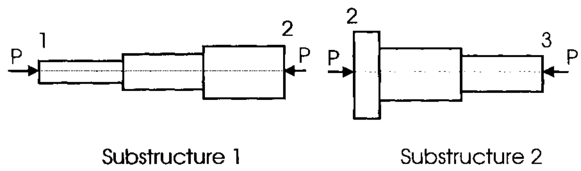

FIGURE 3(b) Substructures of the rotor shown in Fig. 3(a).

strained global dynamic stiffness matrix is 12 × 12 in our case. After introducing the boundary conditions at both ends, one finally obtains the dynamic equilibrium equation:

$$\begin{pmatrix} M_{1x} \\ M_{1y} \\ F_{2x} \\ F_{2y} \\ M_{2x} \\ M_{2y} \\ M_{3x} \\ M_{3y} \end{pmatrix} = [D_g]_{8\times 8} \begin{pmatrix} \theta_{1x} \\ \theta_{1y} \\ X_2 \\ Y_2 \\ \theta_{2x} \\ \theta_{2y} \\ \theta_{3x} \\ \theta_{3y} \end{pmatrix} \quad (15)$$

where $[D_g]$ is the restrained global dynamic stiffness matrix. The unwanted DOF θ_{1x}, θ_{1y}, θ_{2x}, θ_{2y}, θ_{3x}, θ_{3y} may be eliminated by solving the linear set of Eqs. (15) and letting their corresponding exciting moments M_{1x}, M_{1y}, M_{2x}, M_{2y}, M_{3x}, M_{3y} be 0. Finally, we obtain:

$$\begin{pmatrix} F_{2x} \\ F_{2y} \end{pmatrix} = [D_2(\omega, \Omega)] \begin{pmatrix} X_2 \\ Y_2 \end{pmatrix}. \quad (16)$$

It is important to note that the system shown in Fig. 3(a) is exactly reduced to 2DOF with displacements X_2 and Y_2 at the disk as generalized coordinates for a given frequency and rotation speed. It is also noted that the reduced dynamic stiffness matrix $[D_2(\omega, \Omega)]$ of the system is both frequency and rotation speed dependent due to the gyroscopic effect. The FRF matrix $H(\omega, \Omega) = [D_2(\omega, \Omega)]^{-1}$ completely determines the dynamic behaviors of the system. The modal parameters can be obtained with ease at this stage.

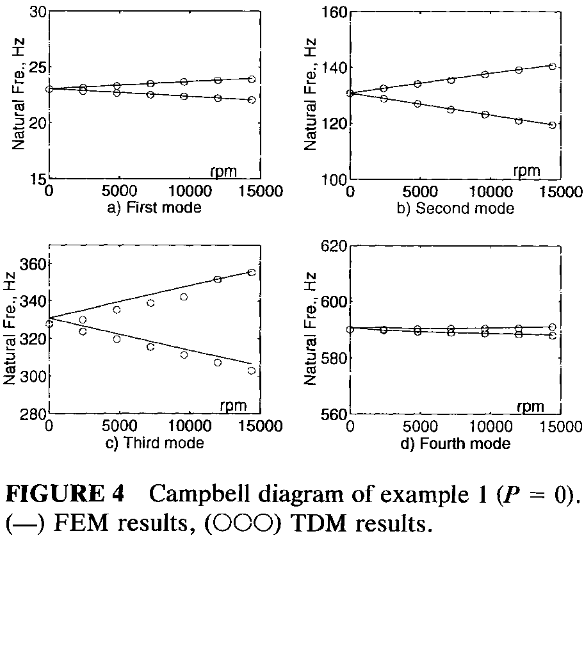

FIGURE 4 Campbell diagram of example 1 (P = 0). (—) FEM results, (OOO) TDM results.

Table 1. Influence of Axial Force on Natural Frequencies (Hz) of Example 1 (ω = 0)

Force (N)	Ω_1	Ω_2	Ω_3	Ω_4
0	22.98	130.74	327.70	590.05
400	22.40	129.96	326.86	589.08
800	21.79	129.16	326.00	588.12
1200	21.16	128.34	325.14	587.16
1600	20.49	127.54	324.28	586.18
2000	19.79	126.70	323.40	585.20
2400	19.05	125.86	322.54	584.20
2800	18.26	125.02	321.66	583.20
3200	17.42	124.16	320.76	582.20
3600	16.52	123.30	319.88	581.18

To validate the correctness of the established model, Fig. 4 depicts the first four natural frequencies predicted by the model as a function of the rotation speed (referred as TDM). For comparison, the finite element (Samcef Software, 20 shaft elements) results (FEM) are also presented in the figure. The influence of the axial force on the natural frequencies is given in Table 1. It is seen that the natural frequencies decrease with the increase of the axial force.

Example 2: Three-Disk and Two-Bearing Rotor

A three-disk and two-bearing rotor system, fixed at one end (Fig. 5) is studied as the second example. The radius of the shaft is 0.025 m. The radius and thickness of the disks are 0.1 and 0.02 m, respectively.

The material of the rotor and disks are steel with Poisson's ratio μ = 0.3, Young's modulus $E = 2.1 \times 10^{11}$ N/m and mass density ρ = 7800 kg/m^3. The two bearings are assumed to be identical and the stiffnesses are:

$$K_{xx} = 1 \times 10^6 \text{ N/m}, \quad K_{yy} = 3 \times 10^6 \text{ N/m}, \quad K_{xy} = K_{yx} = 0.$$

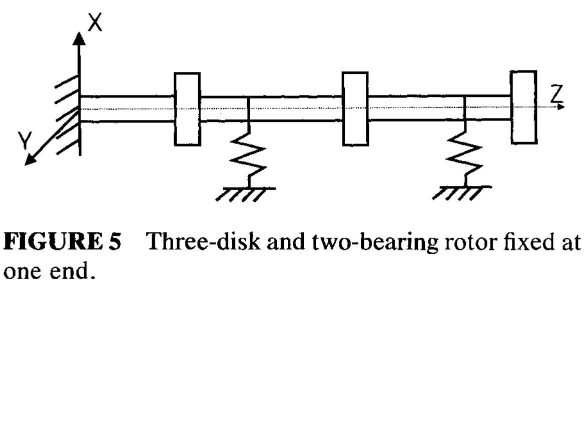

FIGURE 5 Three-disk and two-bearing rotor fixed at one end.

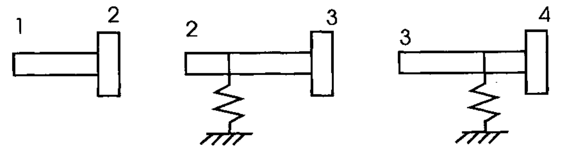

FIGURE 6 Substructures of the rotor shown in Fig. 5.

The rotation speed of the rotor ranges from 0 to 30,000 rpm. The objective is to reduce the system to 6DOF with the translational displacements at disk 1, disk 2, and disk 3 as its generalized coordinates. The 10 basic elements (five shaft elements, two bearing elements, and three disk elements) may be represented by three substructures as shown in Fig. 6.

The dynamic stiffness matrix for each substructure may be obtained from the corresponding transfer matrix. The global dynamic stiffness matrix $[D]$ for the entire rotor system may then be obtained by applying the standard assembly procedure of the FEM. It is noted that the obtained unrestrained global dynamic stiffness matrix is 16×16 in this case. After introducing the boundary conditions at both ends, one finally obtains the dynamic equilibrium equation:

$$\begin{pmatrix} F_{2x} \\ F_{2y} \\ M_{2x} \\ M_{2y} \\ F_{3x} \\ F_{3y} \\ M_{3x} \\ M_{3y} \\ F_{4x} \\ F_{4y} \\ M_{4x} \\ M_{4y} \end{pmatrix} = [D_g]_{12\times 12} \begin{pmatrix} X_2 \\ Y_2 \\ \theta_{2x} \\ \theta_{2y} \\ X_3 \\ Y_3 \\ \theta_{3x} \\ \theta_{3y} \\ X_4 \\ Y_4 \\ \theta_{4x} \\ \theta_{4y} \end{pmatrix} \tag{17}$$

where $[D_g]$ is the restrained global dynamic stiffness matrix.

The unwanted DOF, $\theta_{ix}, \theta_{iy}, i = 2, 3, 4$ may be removed by solving the linear set of Eqs. (17) and setting their corresponding exciting moments $M_{ix}, M_{iy}, i = 2, 3, 4$ to 0. Finally, we obtain:

$$\begin{pmatrix} F_{2x} \\ F_{2y} \\ F_{3x} \\ F_{3y} \\ F_{4x} \\ F_{4y} \end{pmatrix} = [D_6(\omega, \Omega)]_{6\times 6} \begin{pmatrix} X_2 \\ Y_2 \\ X_3 \\ Y_3 \\ X_4 \\ Y_4 \end{pmatrix}. \tag{18}$$

Table 2. Eigenfrequencies (Hz) Obtained by Different Methods (ω = 0)

Mode No.	Ω_1	Ω_2	Ω_3	Ω_4
FEM	53.71	83.96	167.51	173.11
TDM	53.60	83.80	166.20	172.10

So far, we have finally established a 6DOF model with the translational displacements at disk 1, disk 2, and disk 3 as its generalized coordinates. It is noted that the elements of matrix $[D_6]$ are both frequency and rotation speed dependent.

The FRF matrix can be easily obtained by inverting the dynamic stiffness matrix $[D_6]$ given in Eq. (18). The modal parameters can easily be obtained using the same procedure as the dynamic stiffness matrix method (Leung, 1980; Leung, 1983) at this stage.

To validate the correctness of the established model, Table 2 gives the natural frequencies predicted by the transfer function matrix $H(\omega, \Omega) = [D_6(\omega, \Omega)]^{-1}$. For comparison, the finite element (Samcef Software, 13 shaft elements) results are also listed. Figure 7 depicts the transfer function (at disk 3) predicted by the established model (TDM model).

CONCLUSIONS

Modeling of rotor-bearing systems by the FEM or the DEM usually results in large stiffness and mass matrices. In order to compare with the experimental model, it is necessary to reduce the

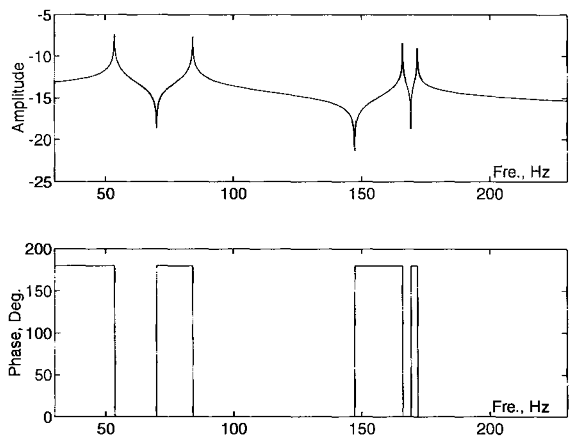

FIGURE 7 Transfer function at disk 3 predicted by the TDM model.

FEM or the DEM model to lower dimension in terms of selected DOF. In this article, an exact and direct modeling technique is presented in which the global dynamic stiffness matrix is obtained directly from the global transfer matrix whose dimension is independent of the number of elements or substructures. Using this method, the rotor-bearing systems can be modeled directly with arbitrary selected DOF. Because the transfer matrix is exact, the global stiffness matrix is also exact. Hence, the results predicted by the model have a higher accuracy than the finite element results.

The method presented is different from the Dokainish combination method. The first difference is that an exact transfer matrix derived directly from the governing equations is used; in Dokainish's method, the transfer matrix was derived from the element stiffness and mass matrices, which are not exact. The second difference, which is the most important difference, is that the Dokainish's method was actually an improved TMM because the eigenproperties were obtained from the global transfer matrix. Only eigenfrequencies, mode shapes, and harmonic responses are available in Dokainish's method. In the present method, the global transfer matrix is transformed to the global dynamic stiffness matrix in terms of which all the modal parameters such as eigenfreqencies, mode shapes, modal masses, modal stiffness, and transfer function can be obtained. Furthermore, any rotor-bearing system can be directly modeled with arbitrary selected DOF. Therefore, the presented method may be considered as an improved dynamic stiffness matrix method.

The authors would like to thank DBS company (Belgium) for the financial support of the project and for the permission to publish this article.

REFERENCES

Chiatti, G., and Sestieri, A., 1979, "Analysis of Static and Dynamic Structural Problems by a Combined Finite Element–Transfer Matrix Method," *Journal of Sound and Vibration*, Vol. 67, pp. 35–42.

Choi, S. H., Pierre, C., and Ulsoy, A. G., 1992, "Consistent Modeling of Rotating Timoshenko Shafts Subject to Axial Loads," *ASME Journal of Vibration and Acoustics*, Vol. 114, pp. 249–259.

Degen, E. E., Shephard, M. S., and Loewy, R. G., 1985, "Combined Finite Element Transfer Matrix Method Based on a Mixed Formulation," *Computers and Structures*, Vol. 20, pp. 173–180.

Dimarogonas, A. D., 1975, "A General Method for Stability Analysis of Rotating Shafts," *Ingenieur-Archiv*, Vol. 44, pp. 9–20.

Dokainish, M. A., 1972, "A New Approach for Plate Vibrations: Combination of Transfer Matrix and Finite-Element Technique," *ASME Journal of Engineering for Industry*, Vol. 94, pp. 526–530.

Fergusson, N. J., and Pilkey, W. D., 1991a, "The Dynamic Stiffness Method: Part 1, Elements," *Shock and Vibration Technology Review*, Vol. 1, pp. 4–13.

Fergusson, N. J., and Pilkey, W. D., 1991b, "The Dynamic Stiffness Method: Part 2, Frequency Extraction Technology," *Shock and Vibration Technology Review*, Vol. 1, pp. 14–20.

Fergusson, N. J., and Pilkey, W. D., 1992, "Frequency-Dependent Element Mass Matrices," *Journal of Applied Mechanics*, Vol. 59, pp. 136–139.

Fergusson, N. J., and Pilkey, W. D., 1993a, "Literature Review of Variants of the Dynamic Stiffness Method, Part 1: The Dynamic Element Method," *Shock and Vibration Digest*, Vol. 25, pp. 3–12.

Fergusson, N. J., and Pilkey, W. D., 1993b, "Literature Review of Variants of the Dynamic Stiffness Method, Part 2: Frequency-Dependent Matrix and Other Corrective Methods," *Shock and Vibration Digest*, Vol. 25, pp. 3–10.

Goodwin, M. J., 1992, "Dynamics of Rotor-Bearing Systems—An Overview," *Shock and Vibration Digest*, Vol. 24, pp. 3–14.

Lee, A. C., Y. Kang, and S. L. Liu, 1991, "A Modified Transfer Matrix Method for Linear Rotor-Bearing Systems," *ASME Journal of Applied Mechanics*, Vol. 58, pp. 776–783.

Leung, A. Y. T., 1980, "Dynamic Analysis of Periodic Structures," *Journal of Sound and Vibration*, Vol. 72, 451–467.

Leung, A. Y. T., and Fergusson, N. J., 1993, "A Generalization of Leung's Theorem," *Proceedings of Dynamics and Design Conference JSME*, July 1993, Tokyo, Japan, Vol. B, paper No. 708, pp. 443–445.

Leung, A. Y. T., and Zhou, W. E., 1993, "Dynamic Stiffness Analysis of Curved Thin-Walled Beams," *Shock and Vibration*, Vol. 1, pp. 77–88.

Lund, J. W., and Orcutt, F. K., 1967, "Calculations and Experiments on the Unbalance Response of a Flexible Rotor," *ASME Journal of Engineering Industry*, Vol. 89, p. 785.

Ohga, M., Shigematsu, T., and Hara, T., 1983, "Structural Analysis by a Combined Finite Element–Transfer Matrix Method," *Computers and Structures*, Vol. 17, pp. 321–326.

Pilkey, W. D., and Fergusson, N. J., 1990, "Some Characteristics of Frequency-Dependent Structural Matrices," *Computers and Structures*, Vol. 35, pp. 413–416.

Richards, T. H., and Leung, Y. T., 1977, "An Accurate Method in Structural Vibration Analysis,"

Journal of Sound and Vibration, Vol. 55, pp. 363–376.
Williams, F. W., and Wittrick, W. H., 1970, "An Automatic Computational Procedure for Calculating Natural Frequencies of Skeletal Structures," International Journal of Mechanical Science, Vol. 12, pp. 781–791.
Wittrick, W. H., and Williams, F. W., 1971, "A General Algorithm for Computing Natural Frequencies of Elastic Structures," *The Quarterly Journal of Mechanics and Applied Mathematics,* Vol. 24, pp. 263–284.
Yang, B. S., and Pilkey, W. D., 1992, "Accurate Approach to Free Vibration Analysis for a Rotating Shaft," *Machine Vibration,* Vol. 1, pp. 164–170.
Zu, J. W. Z., and Han, R. P. S., 1992, "Natural Frequencies and Normal Modes of a Spinning Timoshenko Beam with General Boundary Conditions," *ASME Journal of Applied Mechanics,* Vol. 59, pp. 197–204.

APPENDIX: Matrices [A] and [N] in Eq. (8)

The nonzero elements of matrix $[A]$ are:

$$A_{11} = 1; \quad A_{23} = 1; \quad A_{27} = \frac{1}{KGA};$$

$$A_{31} = \frac{\rho\Omega^2}{KG}; \quad A_{35} = \frac{1}{EI}; \quad A_{43} = b;$$

$$A_{44} = \frac{2\rho\omega\Omega}{E}; \quad A_{47} = a; \quad A_{52} = 1; \quad A_{64} = 1;$$

$$A_{68} = \frac{1}{KGA}; \quad A_{72} = \frac{\rho\Omega^2}{KG}; \quad A_{76} = \frac{1}{EI};$$

$$A_{83} = \frac{-2\rho\omega\Omega}{E}; \quad A_{84} = b; \quad A_{88} = a;$$

with

$$a = \frac{1}{EI} - \frac{\rho\Omega^2}{KGA}\left(\frac{1}{E} - \frac{1}{KG}\right); \quad b = \frac{\rho\Omega^2}{KG} - \frac{\rho\Omega^2}{E};$$

the other elements being equal to 0.

Matrix $[N]$ is obtained as follows:

$$[N] = [H_b][M_b]^{-1}.$$

The matrix $[H_b]$ takes the form

$$[H_b] = \begin{pmatrix} H_1 & H_2 \\ H_1 & -H_2 \end{pmatrix}$$

with the submatrices $[H_1]$, $[H_2]$

$$[H_1] = \begin{pmatrix} C_1 & C_2 & C_3 & C_4 \\ \lambda_a C_2 & \lambda_a C_1 & -\lambda_b C_4 & \lambda_b C_3 \\ \lambda_a^2 C_1 & \lambda_a^2 C_2 & -\lambda_b^2 C_3 & \lambda_b^2 C_4 \\ \lambda_a^3 C_2 & \lambda_a^3 C_1 & \lambda_b^3 C_4 & -\lambda_b^3 C_3 \end{pmatrix}$$

$$[H_2] = \begin{pmatrix} C_5 & C_6 & C_7 & C_8 \\ \lambda_c C_6 & \lambda_c C_5 & -\lambda_d C_8 & \lambda_d C_7 \\ \lambda_c^2 C_5 & \lambda_c^2 C_6 & -\lambda_d^2 C_7 & \lambda_d^2 C_8 \\ \lambda_c^3 C_6 & \lambda_c^3 C_5 & \lambda_d^3 C_8 & -\lambda_d^3 C_7 \end{pmatrix}$$

where C_i, $i = 1, 8$, are constants

$$C_1 = \cosh \lambda_a L, \quad C_2 = \sinh \lambda_a L,$$
$$C_3 = \cos \lambda_b L, \quad C_4 = \sin \lambda_b L$$

$$C_5 = \cosh \lambda_c L, \quad C_6 = \sinh \lambda_c L,$$
$$C_7 = \cos \lambda_d L, \quad C_8 = \sin \lambda_d L$$

and λ_a, λ_b, λ_c, λ_d are the roots of Eq. (5).

The matrix $[M_b]$ is similarly given by:

$$[M_b] = \begin{pmatrix} M_1 & M_2 \\ M_1 & -M_2 \end{pmatrix}$$

with the submatrices $[M_1]$, $[M_2]$

$$[M_1] = \begin{pmatrix} 1 & 0 & 1 & 0 \\ 0 & \lambda_a & 0 & \lambda_b \\ \lambda_a^2 & 0 & -\lambda_b^2 & 0 \\ 0 & \lambda_a^3 & 0 & -\lambda_b^3 \end{pmatrix}$$

$$[M_2] = \begin{pmatrix} 1 & 0 & 1 & 0 \\ 0 & \lambda_c & 0 & \lambda_d \\ \lambda_c^2 & 0 & -\lambda_d^2 & 0 \\ 0 & \lambda_c^3 & 0 & -\lambda_d^3 \end{pmatrix}$$

As a by-product, the exact dynamic stiffness matrix $[D]$ for a rotating shaft subject to axial force can be obtained by rearranging the transfer matrix $[T]$ using Eq. (11) in the text.